

# Kinetic Parameters Determination of Benzene Vapor Adsorption on Activated Carbon Using Differential Permeation Technique

**Aswati Mindaryani**

**Boma W. Tyoso**

**Wahyudi B. Sediawan**

**Supranto**

*Chemical Engineering Department*

*Gadjah Mada University*

*Bulaksumur, Yogyakarta 55281 INDONESIA*

*Email: amindaryani@chemeng.ugm.ac.id*

Equilibrium and kinetic data are very important for a reliable design of a large-scale adsorption system. The objective of the research was to determine the particle scale kinetic parameters of strongly adsorbed volatile organic compounds (VOCs) in activated carbon (AC) by using the differential permeation technique. The experimental rig consisted basically of upstream and downstream reservoirs separated by a slab-shaped AC that is 2 mm thick. After cleaning the slab overnight at 400 K and under vacuum condition, the experiment was started by opening the valve to allow vapor to diffuse through the AC. The upstream and downstream pressures were continuously recorded until equilibrium was reached. Another experiment was run by increasing incrementally the upstream pressure. The same experiment was carried out using nonadsorbed gas (argon) to estimate both Knudsen permeability and viscous permeability. The Knudsen, viscous, and surface diffusivities were determined by matching the total permeability against the experimental data. From the data obtained, it was found that both porosity and surface diffusivity change with loading. The surface diffusivity of benzene vapor in AC pores does not follow the Darken model, but it follows the hydrodynamic model of Gilliland, especially when the porosity is relatively constant at high loading.

**Keywords:** Adsorption, benzene, differential permeation, kinetic, and volatile organic compounds (VOCs).

## INTRODUCTION

The discharge of volatile organic compounds (VOCs) into the atmosphere is an important environmental issue because they may contain aromatic vapors, such as benzene, which are carcinogenic to humans.

Adsorption is a promising method to control the emission of VOCs and, because of their high

affinity for hydrocarbons, activated carbons (ACs) are useful for removing aromatics.

Equilibrium and kinetic data are very important to the reliable design of a large-scale system adsorber.

The objective of this research was to determine the particle scale kinetic parameters of strongly adsorbed VOCs in ACs using the differential permeation technique.

## THEORY

The system consists of a porous particle (adsorbent) mounted between two reservoirs. The mass transfer from one reservoir to the other is affected by the diffusion and flow through the porous particle. A transient mathematical model describing the mass transfer through the particle was formulated. The combined effects of Knudsen, viscous, and surface diffusions contributed to the process.

Prasetyo et al. (2002) used the same technique to determine the hydrocarbon surface diffusion for propane, n-butane, and n-hexane and observed that under differential condition the effect of heat was very minimal; therefore, the system could be maintained isothermally. The mathematical model for isothermal system was formulated as follows:

$$\varepsilon \frac{\partial}{\partial t} \left( \frac{P}{RT} \right) + (1-\varepsilon) \frac{\partial C_\mu}{\partial t} = \frac{\partial}{\partial z} \left[ \varepsilon \frac{D_p}{RT} \frac{\partial P}{\partial z} + \varepsilon \frac{B_o P}{\mu RT} \frac{\partial P}{\partial z} + (1-\varepsilon) D_\mu \frac{\partial C_\mu}{\partial z} \right] \quad (1)$$

The effect of finite mass exchange between the phases on the overall kinetics of adsorption had also studied and it was found that, for particle sizes greater than 1 mm, the local equilibrium assumption was valid (Do and Wang 1998a, 1998b). The isotherm of benzene at 298 K can be presented by Toth equation (Prasetyo 2000):

$$C_\mu = 11225 \frac{0.2 P}{[1 + (0.2 P)^{0.31}]^{1/0.31}} \quad (2)$$

For adsorbents with constricted pores, such as carbon molecular sieves, the local equilibrium assumption may not hold (Nguyen and Do 2000). The pressures at the two end faces of the particle can be described by the following mass balance equations:

$$\frac{d}{dt} \left( \frac{V_1 P_1}{RT} \right) = A \left[ \varepsilon \frac{D_p}{RT} \frac{\partial P}{\partial z} + \varepsilon \frac{B_o P}{\mu RT} \frac{\partial P}{\partial z} + (1-\varepsilon) D_\mu \frac{\partial C_\mu}{\partial z} \right] \quad (3)$$

$$\frac{d}{dt} \left( \frac{V_2 P_2}{RT} \right) = -A \left[ \varepsilon \frac{D_p}{RT} \frac{\partial P}{\partial z} + \varepsilon \frac{B_o P}{\mu RT} \frac{\partial P}{\partial z} + (1-\varepsilon) D_\mu \frac{\partial C_\mu}{\partial z} \right]_{z=l} \quad (4)$$

The upstream reservoir pressure was essentially constant throughout the experiment because of its large volume ( $5 \times 10^{-3} \text{ m}^3$ ) compared with that in the downstream reservoir ( $38.9 \times 10^{-6} \text{ m}^3$ ). Thus, Eq. (3) was simplified to:

$$P|_{z=0} = P_1, \dots \quad (5)$$

with the initial condition:

$$t = 0, P = P_i, \dots \quad (6)$$

The differential equation was solved numerically, the result being  $P_2$  as a function of time. Porosity and surface diffusivity were determined by matching the simulation breakthrough against the experimental data. Although  $D_p$  and  $B_o$  were determined from the argon experiment, other gases could be calculated from:

$$\frac{D_p}{D_{p,Ar}} = \sqrt{\frac{M_{Ar} \cdot T_{Ar}}{MT}} \quad (7)$$

## EXPERIMENTAL

The sample cell was a slab-shaped Ajax type 976 ( $L = 2 \times 10^{-3} \text{ m}$ ), prepared by coating the cylindrical surface with strong epoxy resin, with a total porosity of 0.71, a macropore porosity of 0.31, and a Brunnauer–Emmett–Teller (BET) surface area of  $1,200 \text{ m}^2/\text{g}$ . The experimental rig is shown in Figure 1.

Before adsorption measurements, the sample cell was degassed under vacuum at 400 K. After cleaning the sample overnight, the rig temperature was set at a desired temperature, and the upstream reservoir was filled with a certain amount of VOC vapor. The experiment started with opening the valve to allow vapor to diffuse through the sample cell. The upstream and downstream pressures

were monitored and recorded into a personal computer using a multichannel data logger. The upstream reservoir pressure was essentially constant throughout the experiment because of its large volume. After the system had reached equilibrium, when the pressures of the upstream and downstream reservoirs became equal, the sample cell was isolated. The time elapsed before reaching equilibrium varied depending on the upstream pressure: the lower the upstream pressure, the longer the equilibrium time.

Another experiment was run increasing incrementally the upstream pressure and allowing the system to reach a new equilibrium. Adsorption was measured within a relative pressure range, from  $10^{-3}$  to 1. The same experiment was carried out using nonadsorbed gas (argon) to estimate the Knudsen and viscous permeabilities. Through the experiment, downstream pressures were monitored versus time,  $P_2 = f(t)$ .

## RESULTS AND DISCUSSION

### Argon experiment

Argon ( $M=40$ ,  $\mu_{298\text{K}}=2.227\text{ Pa}\cdot\text{s}$ ) was used to estimate the Knudsen and viscous diffusivities. From the data for downstream pressure versus

time for several pressures,  $D_{pAr}=4.77\times 10^{-5}\text{ m}^2/\text{s}$  and  $B_o=3\times 10^{-15}\text{ m}^2\cdot\text{Pa}$ . Those for benzene were calculated using Eq. (7) and the results were  $D_{pBz}=3.2\times 10^{-5}\text{ m}^2/\text{s}$  and  $B_o=3\times 10^{-15}\text{ m}^2\cdot\text{Pa}$ .

### Benzene experiment

From the experimental data, porosity ( $\epsilon$ ) and surface diffusivity ( $D\mu$ ) can be determined. Table 1 shows that average errors are acceptable; therefore, both isothermal and local equilibrium assumptions hold. For the first data, error was at 36 % because of the pressure transducer's sensitivity; at very low pressure, the error would be much higher than at higher pressures.

### Porosity

The porosity of a particle changes with surface concentration, as shown in Figure 2. The higher the surface concentration, the more occupied the micropore, hence, the smaller the porosity. This can be represented by Eq. (8). The porosity for benzene adsorption decreased sharply with loadings started at 0.53. The adsorption started with micropore utilization and, at higher loadings, the macropore could be utilized and the porosity became constant at  $\epsilon = 0.072$ .

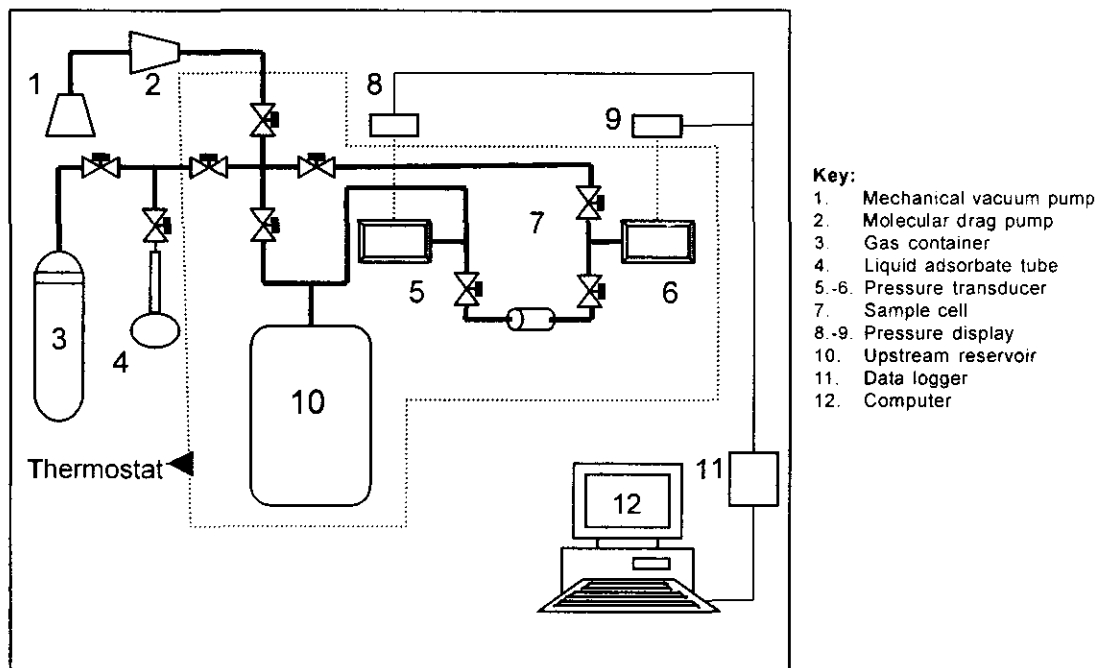
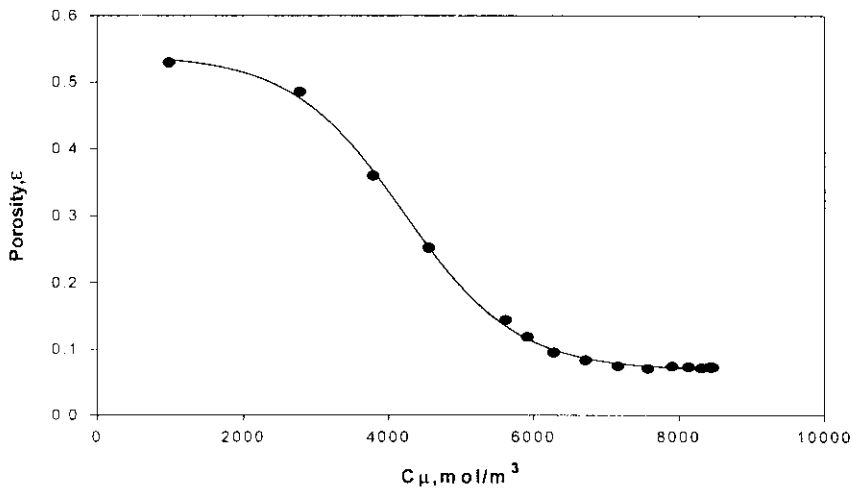


Figure 1. Schematic Diagram of Experimental Rig

**Table 1. Porosity and Surface Diffusivity at Various Loadings**

Pav,Pa	P/Po	C $_{\mu}$ Mol/m <sup>3</sup>	Porosity	D $_{\mu}$ ,10 <sup>14</sup> m <sup>2</sup> /s	Error %
3.373	0.000264	979.578	0.52914	0.03	36.7
36.123	0.002822	2777.954	0.48500	1470.00	4.90
95.593	0.007469	3785.912	0.35914	1771.80	1.28
191.675	0.014976	4551.453	0.25167	3167.24	1.80
501.342	0.039171	5612.845	0.14384	3982.00	0.45
661.0035	0.051646	5910.296	0.11836	3966.40	1.40
935.500	0.073093	6275.333	0.09488	6104.00	0.62
1446.671	0.113032	6716.726	0.08300	7840.00	1.50
2297.480	0.179509	7161.014	0.07400	8200.00	0.84
3640.412	0.284436	7575.608	0.07062	10020.00	0.73
5424.294	0.423815	7911.144	0.07400	11000.97	0.30
7188.032	0.561621	8134.404	0.07274	12006.61	0.25
9104.266	0.711342	8313.047	0.07140	13000.33	0.16
10584.100	0.826965	8422.727	0.07240	12491.80	0.05
11326.000	0.884932	8471.011	0.07220	12002.88	0.29



**Figure 2. Porosity at Various Loadings**

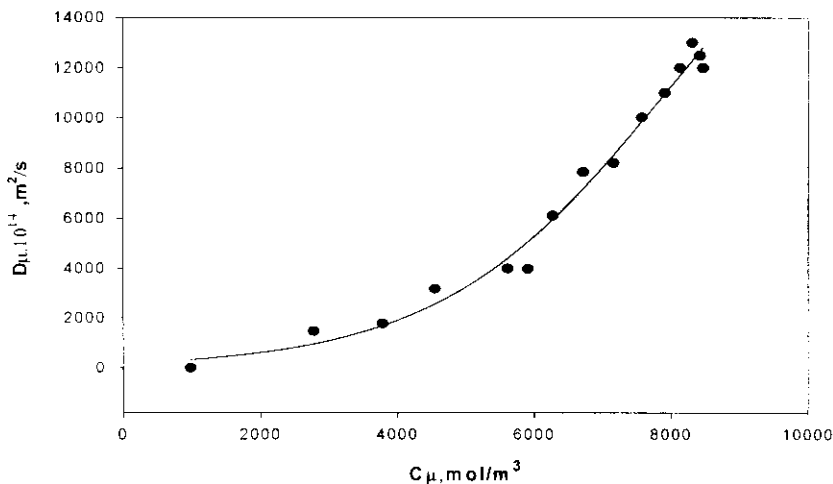


**Figure 3. Surface Diffusivity at Various Loadings**

$$\epsilon = 0.0675 + \frac{0.4727}{1 + \exp\left[\frac{C_\mu - 4204.6}{790.8}\right]} \quad (8)$$

with the correlation coefficient of 0.99.

**Surface diffusivity**

In Figure 3, the surface diffusivity is shown to increase up to a loading of 8,300 mol/m<sup>3</sup>, beyond which it exhibits a sharp decrease due to the decrease of porosity observed in Figure 2.

The surface diffusivity in the region of loadings less than 8,300 mol/m<sup>3</sup>, can be correlated by the following equation:

$$D_\mu = -1427 + (1051) \text{Exp}(3.31 \times 10^{-4} C_\mu) \quad (9)$$

The correlation coefficient is 0.992. The surface diffusivity values from this experiment were comparable to those obtained from the measurement using the constant molar flow rate (Prasetyo et al. 2002).

According to Darken, surface diffusivity at any loading is equal to the value at zero loading multiplied by a thermodynamic correction factor (Do 1998):

$$D_\mu = D_\mu^* \frac{\partial \ln P}{\partial \ln C_\mu} \quad (10)$$

Should the plot of  $D_\mu$  versus  $\frac{\partial \ln P}{\partial \ln C_\mu}$  give a straight line, the slope would be the constant corrected diffusivity  $D_\mu^*$ . However, as shown in Figure 4, this plot cannot be described by a straight line, suggesting that the corrected diffusivity is not constant, but rather increasing with loading.

Hence, surface diffusivity of benzene does not follow the Darken model, which usually can be applied at sub-monolayer, at low coverage, with high interaction between the adsorbed phase and the solid surface. This experiment had a very high range coverage, up to 8,300 mol/m<sup>3</sup>. At high coverage, the adsorbate occupied the lower energy level; therefore, the interaction between the adsorbed phase and the solid surface was not strong.

Based on the hydrodynamic model of Gilliland, which regards the adsorbed gas phase as a laminar flowing film of viscous liquid (Gilliland et al. 1974),

$$B_\mu = (1 - \epsilon) D_\mu \frac{\partial C_\mu}{\partial P} = k \frac{C_\mu^2}{P} \quad (11)$$

$\frac{\partial C_\mu}{\partial P}$  is the gradient of isotherm at average pressure. From Figure 5, it can be seen that the plot of  $B_\mu$  versus  $\frac{C_\mu^2}{P}$  is relatively linear, except when the benzene loading is very low.

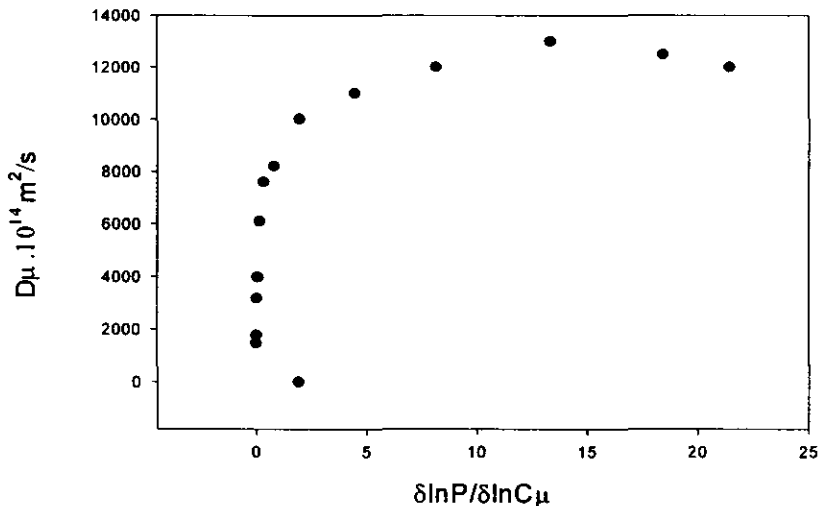


Figure 4.  $D_\mu$  versus  $\frac{\partial \ln P}{\partial \ln C_\mu}$

At higher loading, the adsorbed gas phase behaves as a laminar flowing film of viscous liquid.

So it is shown that when the porosity is almost constant, the surface diffusivity of benzene vapor in activated carbon pores follows the hydrodynamic model of Gilliland and the correlation is:

$$B\mu = 85.8 + 0.094 \frac{C_{\mu}^2}{P} \quad (12)$$

with the correlation coefficient of 0.963.

## CONCLUSIONS

The isothermal model represents the differential permeation process very well.

Results show that adsorption starts with micropore utilization and, at higher loading, the macropore can be utilized. The porosity for benzene adsorption starts from 0.53 and continues until the porosity becomes constant at  $\varepsilon = 0.072$ . Hence, porosity decreases sharply with loadings.

Surface diffusivity, however, increases with loading until  $C_{\mu} = 8,300 \text{ mol/m}^3$  and decreases as the pores are fully occupied by the adsorbed phase. The surface diffusivity of benzene vapor in AC pores follows the hydrodynamic model of Gilliland and not the Darken model.

## NOMENCLATURE

$B_0$	viscous flow parameter, $m^2 \cdot Pa$
$C_{\mu}$	adsorbed phase concentration, $mol/m^3$ of solid
$D_p, D_{\mu}$	Knudsen diffusivity, surface diffusivity, $m^2/s$
$L$	particle length, $m$
$M$	molecular weight, $kg/mol$
$P_1, P_2$	upstream and downstream reservoir pressure, $Pa$
$P, P_i, P_0$	intraparticle, initial, and vapor pressures, $Pa$
$T$	temperature, $K$
$t$	time, $s$
$V_1, V_2$	upstream

and downstream reservoir volume,  $m^3$

$z$	position, $m$
$\mu$	fluid viscosity, $Pa \cdot s$

## ACKNOWLEDGMENT

The work presented in this paper was carried out at the Adsorption Science and Reaction Engineering Laboratory, Chemical Engineering Department, University of Queensland, Australia, under the supervision of Prof. D. D. Do and with the financial support of the QUE Project, Chemical Engineering Department, Gadjah Mada University, Indonesia. They are gratefully acknowledged.

## REFERENCES

- Do, D. D. (1998). *Adsorption analysis: Equilibria and kinetics*, Imperial College Press, London.
- Do, D. D., and Wang, K. (1998a). "A new kinetic model for the description of adsorption kinetics in heterogeneous activated carbon," *Carbon*, 36, 1539.
- Do, D. D., and Wang, K. (1998b). "Dual diffusion and finite mass exchange model for adsorption kinetics in activated carbon," *AIChE J.*, 44, 68.
- Gilliland, E., Baddour, R. F., Perkinson, G. P., and Sladek, K. J. (1974). "Diffusion on surfaces: Effect of concentration on the diffusivity of physically adsorbed gases," *Ind. Eng. Chem. Fundam.*, 13, 2, 99-100.
- Nguyen, C., and Do, D. D. (2000). "A dual Langmuir kinetic model for adsorption in carbon molecular sieve materials," *Langmuir*, 16, 1868.
- Prasetyo, I. (2000). *Kinetics characterization of hydrocarbons on activated carbon with new constant molar flow and differential permeation techniques*, Ph.D. Thesis, University of Queensland, Australia.
- Prasetyo, I., and Do, D. D. (1999). "Adsorption kinetics of light paraffins in activated carbon by a semi-batch constant molar flow rate method," *A.I.Ch.E. Journal*, 45, 8, 1892-1900.

Prasetyo, I., Do, H. D., and Do, D. D. (2002).  
"Surface diffusion of strong adsorbing  
vapors on porous carbon," *Chemical  
Engineering Science*, 57, 11-141.